Vol 11 No 4, April 2002
1009-1963/2002/11(04)/0358-08

Chinese Physics

© 2002 Chin. Phys. Soc.
and IOP Publishing Ltd

# Two-phase flow in correlated pore-throat random porous media*

Tian Ju-Ping(田巨平)[a] and Yao Kai-Lun(姚凯伦)[b]

[a] *Department of Physics, Wuhan Institute of Science and Technology, Wuhan* 430073, *China*

[b] *Department of Physics Huazhong University of Science and Technology, Wuhan* 430074, *China;*
*CCAST (World Laboratory), Beijing* 100080, *China*

[b] *International Center for Material Physics, Chinese Academy of Science, Shenyang* 110015, *China*

(Received 10 June 2001; revised manuscript received 9 December 2001)

We have constructed a porous media model in which there are percolation clusters with varying percolation probability $P$ and correlated site-bonds. Taking into account both the pore and the throat geometry, the viscous fingering (VF) in porous media has been investigated by using the standard over-relaxed Gauss–Seidel scheme. The simulation results show that the VF structure varies with the correlation parameter $\varepsilon$, the viscosity ratio $M$ and the percolation probability $P$. The smaller the correlation parameter $\varepsilon$, the greater the deviation of the normalized size distribution of the invaded throat $N_{\rm inv}(r)$ from the truncated Rayleigh distribution. For a larger viscosity ratio $M$, the VF pattern looks like a diffusion-limited-aggregation structure in percolation clusters. The fractal dimension $D$ increases with the increase of the percolation probability $P$ and the correlation parameter $\varepsilon$. The velocity distribution $f(\alpha)$ of VF in percolation clusters is of a parabola-like curve. The tail of the distribution (large $\alpha$) is longer for a larger correlation parameter $\varepsilon$. For a smaller $\varepsilon$, the distribution is very sharp. The sweep efficiency $E$ decreases along with the decrease of the correlation parameter $\varepsilon$ and the increase of the network size $L_{\rm nz}$. $E$ has a minimum as $L_{\rm nz}$ increases up to the maximum no matter what the values of $P$, $M$ and $\varepsilon$. The $E \sim L_{\rm nz}$ curve has a frozen zone and an active zone. The geometry and the topology of the porous media have strong effects on the displacement processes and the structure of VF.

**Keywords:** correlation parameter, fractal dimension, sweep efficiency, scaling function
**PACC:** 4755M, 6780

## 1. Introduction

Viscous fingering (VF) in porous media has been extensively studied in the past years, and recently it has become a very active research field. This phenomenon is also of practical importance in the recovery of oil. The displacement of viscous oil by a less viscous solvent is inherently unstable. Even when the porous media are homogeneous, a VF will still form, and reduce the sweep efficiency, thus leading to an early breakthrough of the injected fluid. Models for simulating VF patterns include mainly: diffusion limited aggregation (DLA),[1] the dielectric breakdown model (DBM),[2] the gradient-governed growth model (GGGM),[3] the two-walker model (TWM),[4] the probabilistic model,[5] DLA with the consideration of surface tension,[6] the shell-by-shell model,[7] the deterministic model,[8−10] and so on. In the deterministic model, the successive over-relaxation technique has been widely employed.[11] In previous works, the geometrical models of deterministic algorithm have been based on a square lattice,[8] a hexagonal lattice[9] or a Sierpinski lattice,[10] a percolation cluster[12] and a percolation cluster with a displacement-freezing-thawing cycle.[13] In particular, reservoir rocks are rarely homogeneous. The porous media flow occurs in a discrete and highly chaotic network of pores and pore throats. Real porous media have a wide range of porosity, or of the concentration of open pores (percolation probability $P$). Murat and Aharony[14] have shown that VF and DLA exhibit many different features in the vicinity of the percolation threshold. These represent a porous medium by a network of interconnected sites (pore) and bonds (throat) in the above-mentioned models. But the volume of pore bodies has been ignored. Ferer *et al.*[15] has taken the pore bodies as unit volume in the square-lattice model. However, in their model, the variation of the pore bodies and the correlation of the pore throat have been ignored. In fact, the radius of the pore is larger than that of the throat, and they (pore and throat)

*Project supported by the Foundation of the Hubei Provincial Education Department, China (Grant No 2000B25002).

are also correlated in real porous media.

In this paper, the variation of percolation clusters with the percolation probability is studied first. The percolation clusters correspond to the connected porous media with the site as pore and the bond as throat. The correlated site–bond model is also constructed for a percolation cluster (see Sec.II). We give a detailed description of the algorithm used in the simulation in Sec.III. VF patterns in percolation clusters are shown in Sec.IV. In Sec.V, the kinetics of the invasion and the fractal dimension of a VF pattern are investigated, the velocity distribution is studied and discussed, and the sweep efficiency of displacement fluid is also discussed. Finally, Sec.VI presents our conclusions.

## 2.Correlated pore-throat model

In a square lattice ($201\times201$) with a given percolation probability $P$, if $P\geq0.59$, a spanning cluster occurs; at $P=1$, the percolation probability for the site reaches 100%. The connectivity of the porous media varies according to the values of $P$. Those sites and clusters beyond the spanning cluster correspond to the non-connection areas of the sedimentary rocks. Our simulation is only concerned with the spanning cluster.

We represent a porous medium by a square network of interconnected sites (pores) and bonds (throats). The radii of those sites beyond the spanning cluster are considered to be zero. The radii of those sites in the spanning cluster are determined by the following construction principle. The radii of the pores are described by a distribution function $f(R)$ while the radius distribution of the throats is given by $g(r)$. In order to build a correlated site–bond network, a construction principle has been built by Vidales *et al.*[16] For a given site, the size is always greater than that of any of its four bonds. In this paper, the pore bodies (sites) and the throats (bonds) are regarded as spherical and cylindrical, respectively (see Sec.III). In order to make our porous media model agree more with the facts, according to the construction principle,[16] the following factor must be considered: among the four bonds connected to a pore, there are at most two bonds with their radii greater than or equal to $\frac{1}{\sqrt{2}}$ of the pore's radius, and they cannot be neighbours. Overlapping of the distribution curves is allowed. This means that there must be some bonds that are greater than some sites. Therefore, when sites and bonds are brought together to form a network, they cannot be chosen independently. The sites and bonds cannot be interconnected completely at random if the construction principle is to be observed. A joint distribution may be defined as $F(R,r)\mathrm{d}R\mathrm{d}r=g(r)f(R)\phi\ (R,r)\mathrm{d}R\mathrm{d}r$, where $F(R,r)\mathrm{d}R\mathrm{d}r$ is the probability of finding a site with a radius in the range $(R,R+\mathrm{d}R)$ connected to a bond with a radius in the range $(r,r+\mathrm{d}r)$. $\phi(R,r)$ is the correlation function characterizing the structure. If $\phi=1$, the sites and bonds are uncorrelated. For $0<\phi<1$, there is a correlation between sites and bonds, and the pores-throat sizes of many porous media satisfy the Rayleigh distribution[16]: $f(r)=2re^{-r^2}$. For simplicity, we assume that the pore and the throat radii follow the truncated Rayleigh distribution,[10] and their maximum radii are $3(1+\varepsilon)$ and 3, and their minimum radii are $3\varepsilon$ and 0, respectively. For the throat and the pore, we set, respectively,

$$g(r)=r\exp(-r^2/2r_m^2)/r_m^2[1-\exp(-3/2r_m^2)],$$
$$(0\leq r\leq 3) \tag{1}$$

$$f(R)=g(R-3\varepsilon),\quad (3\varepsilon\leq R\leq 3(1+\varepsilon)) \tag{2}$$

where $r_m$ is the most probable radius of the throat, and $\varepsilon$ $(0<\varepsilon\leq1)$ is a correlation parameter, which shows the correlation characteristic between sites and bonds. We set the most probable radius of the throat $(r_m)$ to be $1/\sqrt{2}$. The distribution form is very common.[17] Figure 1 shows the three situations of the distribution of the site and bond radii. It is obvious that the overlap between the pore and the throat radii distributions is zero when $\varepsilon\geq1$, indicating that the site and bond are uncorrelated; whereas the site and bond are strongly correlated when $\varepsilon\approx0$. Therefore, the radii of the sites and their attached bonds are assigned according to the construction principle.

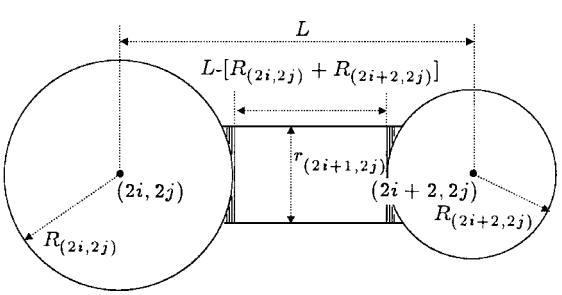



**Fig.1.** Two spheres in two neighbouring lattices $(2i,2j)$ and $(2i+2,2j)$ connected by a cylindrical throat. Their radii are chosen randomly according to Eqs.(1) and (2) and the construction principle.

## 3. Simulation method

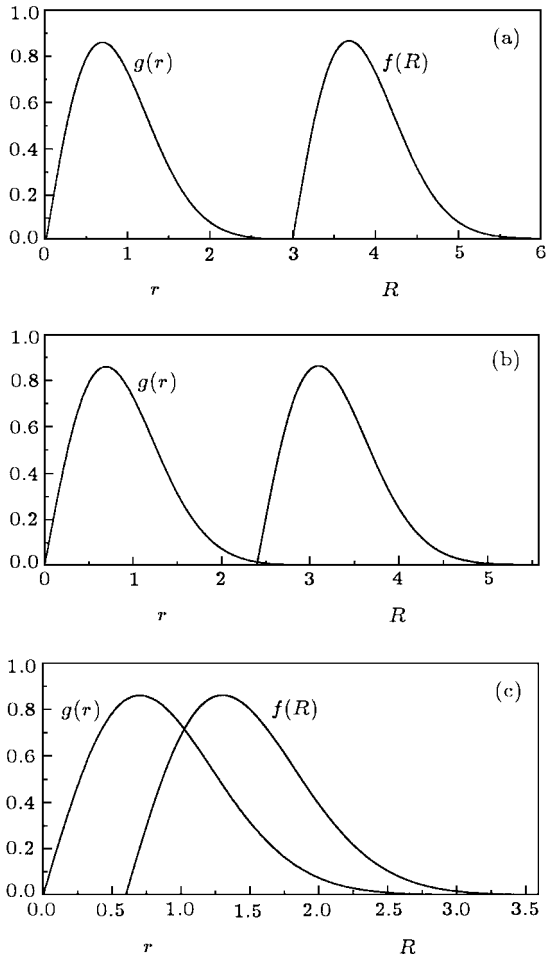



**Fig.2.** The pore-throat distribution function: (a) $\varepsilon$=1; (b) $\varepsilon$=0.8; (c) $\varepsilon$=0.2.

To ascertain the effects of the correlated pore throats, we model a two-dimensional porous medium by a $L_x \times L_y$ square lattice (we choose $L_x = L_y$=201). This square lattice model has pore bodies with varying radii according to Eq.(1), at the lattice sites $\boldsymbol{z} = (2i, 2j)$ for integers $i = 1 \to L_x$, and $j = 1 \to L_y$. These pore bodies are considered to be spheres, connected by cylindrical throats, at the vertical and horizontal bond locations $\boldsymbol{z} = (2i+1, 2j)$ and $\boldsymbol{z} = (2i, 2j+1)$, respectively. The radii of all the throats are chosen randomly according to Eq.(2) and the construction principle (see Fig.2). It is obvious that our model is different from that in Refs.[8]–[10], in which the pore volume was not taken into account. Our model is also different from that in Ref.[15] which takes the pore bodies as unit volume and considers the throat radii to be uniformly distributed in the interval of 0 to 1. On the basis of the above-mentioned model, the volume of the pore body at a lattice site $\boldsymbol{z} = (2i, 2j)$ is (see Fig.1)

$$\begin{aligned} V_{(2i,2j)} =& \frac{4}{3}\pi R^3_{(2i,2j)} + \sum_k \Bigg\{ \pi r^2_{(2i,2j)+k}(R_{(2i,2j)} \\ & - \sqrt{R^2_{(2i,2j)} - r^2_{(2i,2j)+k}}) \\ & - \left[\frac{2}{3}\pi R^3_{(2i,2j)}(1 - \sqrt{1 - r^2_{(2i,2j)+k}/R^2_{(2i,2j)}})\right] \\ & - \frac{1}{3}\pi r^2_{(2i,2j)+k}\sqrt{R^2_{(2i,2j)} - r^2_{(2i,2j)+k}}\Bigg\}. \end{aligned} \quad (3)$$

where $R_{(2i,2j)}$ is the radius of the lattice site $\boldsymbol{z} = (2i, 2j)$, and $r_{(2i+1,2j)}$ is the radius of the bond $(2i+1, 2j)$. $\boldsymbol{k}$ can be (1,0), (-1,0), (0,1) and (0,-1). We assume Poiseuille fluid flow through a throat, neglecting the surface tension effects on the capillary pressure and wetting.[15] Hence at the volume flow rate $q$, the pressure drop ($\Delta P$) across the throat at $\boldsymbol{z} = (2i+1, 2j)$ is

$$\Delta P_{(2i+1,2j)} = q_{(2i+1,2j)}/T_{(2i+1,2j)}, \quad (4)$$

where $\Delta P_{(2i+1,2j)} = P_{(2i,2j)} - P_{(2i+2,2j)}$, $P_{(2i,2j)}$ and $P_{(2i+2,2j)}$ are the pressures at the $(2i, 2j)$th and $(2i+2, 2j)$th nodes, respectively, $T_{(2i+1,2j)} (= \pi r^4_{(2i+1,2j)}/8 [\mu_1 x_{(2i+1,2j)} + \mu_2 (l_{(2i+1,2j)} - x_{(2i+1,2j)})])$ is the conductance of the throat, $\mu_1$ and $\mu_2$ are the viscosities of the injected and displaced fluids, $M = \mu_2/\mu_1$ is the viscosity ratio, $x_{(2i+1,2j)}$ is the length of bond $(2i+1, 2j)$ occupied by the injected fluid, and $l_{(2i+1,2j)}$ is the length of bond $(2i+1, 2j)$. $l_{(2i+1,2j)} = L - (R_{(2i,2j)} + R_{(2i+2,2j)})$, where $L$ is the distance between the two lattice sites $(2i, 2j)$ and $(2i+2, 2j)$. In this paper $L$ is chosen to be four times larger than that of the maximum pore radius. At each node we have the conservation equation

$$\sum_k q_{(2i,2j)+k} = 0. \quad (5)$$

Using Eq.(4) in this conservation equation, we find a discretized Laplace equation[15]

$$P_{(2i,2j)} = \sum_k T_{(2i,2j)+k} P_{(2i,2j)+2k} / \sum_k T_{(2i,2j)+k}. \quad (6)$$

We have chosen boundary conditions with a high pressure ($P$=100) at the central pore body and zero pressure at the outlet edge. To find iterative solutions for the pressure field, we have used the standard over-relaxed Gauss–Seidel scheme so that the normalized residuals $\mathcal{R}$[15]

$$\mathcal{R} = \sum_{i,j} \left\{ \sum_k q_{(2i,2j)+k} \Big/ \sum_k T_{(2i,2j)+k} \right\}^2 \quad (7)$$

Fall below a confidence limit, which we normally choose to be $10^{-5}$. Next, we use Eq.(6) to determine the pressure field, the pressure drop across the throat and the conductance. The flow rate in each throat can be determined by using Poiseuille's law (Eq.(4)). Then a straightforward deterministic procedure is used to advance the interface through a short time $\Delta t$. We choose a value of $\Delta t$ such that the interface advances a quarter of the pore-body volume in that interface throat with the maximum volume flow rate, i.e. $q_{\max}\Delta t=1/4$. The flow rules allow the interface to advance through throats such that the flow is from a fully invaded pore body towards a pore body which is not yet fully invaded. The flow is allowed in every throat, and the deterministic flow velocity is allowed to advance or retreat the interface within the pore throat.

## 4. VF Patterns and evolution of the porous media

Figure 3 shows the VF pattern in a percolation cluster ($P$=0.8 and $M$=100) for four different correlation parameters ($\varepsilon$=1, 0.8, 0.6, 0.2). For $\varepsilon$=1, the VF pattern has been studied.[12] For $\varepsilon$ <1, the cluster size decreases with the decrease of the correlation parameter $\varepsilon$ (see Fig.3). We also find that the VF pattern remains almost unchanged when $\varepsilon \geq 1$. Moreover, no matter what value $\varepsilon$ takes, the VF pattern in the percolation cluster is of an anisotropy manner.

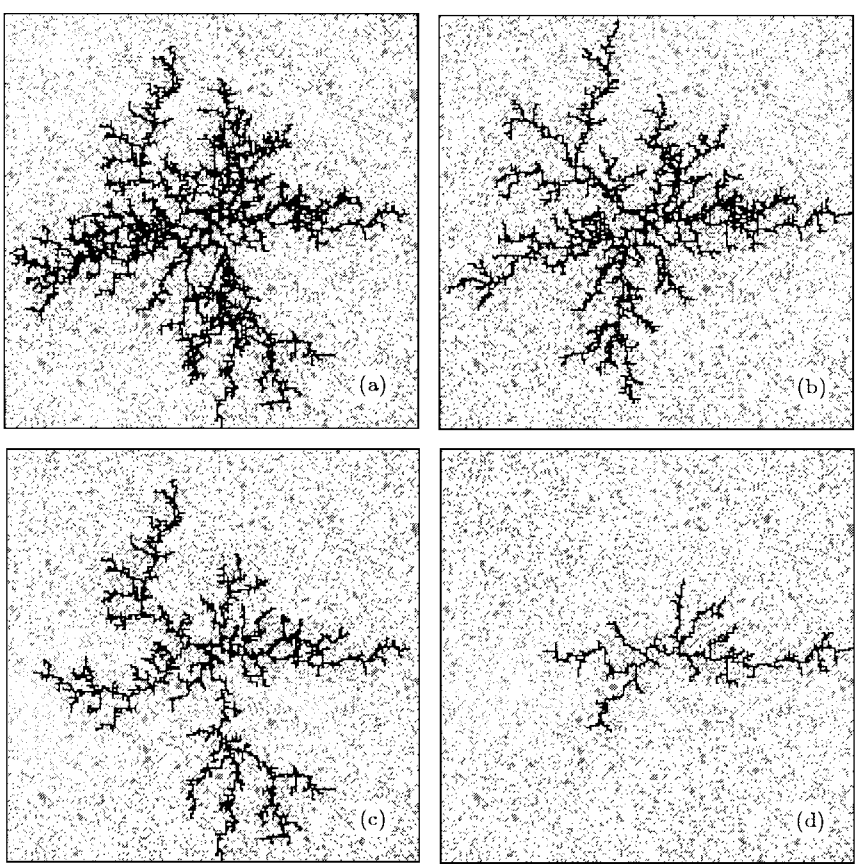



**Fig.3.** VF pattern in a percolation cluster for four different correlation parameters ($\varepsilon$=1(a), 0.8(b), 0.6(c), 0.2(d)). $P$=0.8 and $M$=100.

Figure 4 presents the normalized size distribution of the invaded throat $N_{\rm inv}(r)$ for correlation parameters $\varepsilon$=0.8(a) and 0.2(b). It is obvious that the smaller the correlation parameter $\varepsilon$, the greater the deviation of the normalized size distribution of the invaded throat $N_{\rm inv}(r)$ from the truncated Rayleigh distribution (Eq.(1)). In Fig.4, the normalized size distribution of the invaded throat, $N_{\rm inv}(r)$, shows that the major deviation happens where $r$ is large. This suggests that the standard over-relaxed Gauss–Seidel

scheme chooses a larger size of throat for displacement. These results are different from the invasion percolation in a square lattice.[11] The reason can be as follows. The invasion percolation model is consistent with the situation at a low capillary number, in which water is injected slowly into a porous medium filled with oil, the capillary force is greater than the viscous force, and the dynamics is determined by the local pore radius $r$. Capillary forces are the strongest at the narrowest pore necks. Hence, the viscous forces are negligible in both fluids, and the principal force is due to capillary action. In every time step the invading fluid advances to the growth site that has the lowest random number $r$. However, our model is a deterministic growth model. In the VF, the principal force is due to the viscosity of the displaced fluid; the viscous forces dominate the capillary force so the capillary effect is negligible. Moreover, according to Eq.(4), the flow conductance $T_{(2i+1,2j)}$ is equal to $\pi r^4_{(2i+1,2j)}/8[\mu_1 x_{(2i+1,2j)} + \mu_2(l_{(2i+1,2j)} - x_{(2i+1,2j)})]$. Hence, the over-relaxation scheme chooses a larger throat size for displacement. Moreover, from Fig.4 we can see that the normalized size distribution of an invaded throat $N_{\rm inv}(r)$ greatly deviates from the truncated Rayleigh distribution when $\varepsilon$ is smaller. The smaller the value of $\varepsilon$, the greater the deviation. This means that there is a strong correlation between the pore and the throat radii.

When $P$=1, for finite values of $M$, such as $1 \leq M \leq 100$, the interior of the cluster of the displacing fluid is compact for short length scales. This structure becomes more and more compact with the decrease of $M$. It is known that the flow pattern will be fractal for infinite viscosity ratio $M$.[18] Our simulation of fluid flow also exhibits fractal for a larger viscosity ratio (i.e. $M$=1000), whether the throat radii are in uniform distribution or truncated Rayleigh distribution. Figure 5 shows the VF pattern for the correlation parameter $\varepsilon$=0.2 and the viscosity ratio $M$=1000 in four different percolation clusters ($P$=0.6, 0.7, 0.8 and 0.9). The simulation result shows that the VF pattern looks like a DLA structure in a percolation cluster. The sweep efficiencies increase with the increase of percolation probability $P$. For varying percolation probability $P$, the numerical relationships between the correlation parameter $\varepsilon$ and fractal dimension $D$ are calculated, as shown in Fig.6. It is clear that the fractal dimension $D$ increases with the increase of the percolation probability $P$ and the correlation parameter $\varepsilon$. This means that VF patterns are fractal no matter what the values of $P$ and $\varepsilon$, for a larger viscosity ratio $M$. Its fractal dimension $D$ also increases with the increase of $P$.

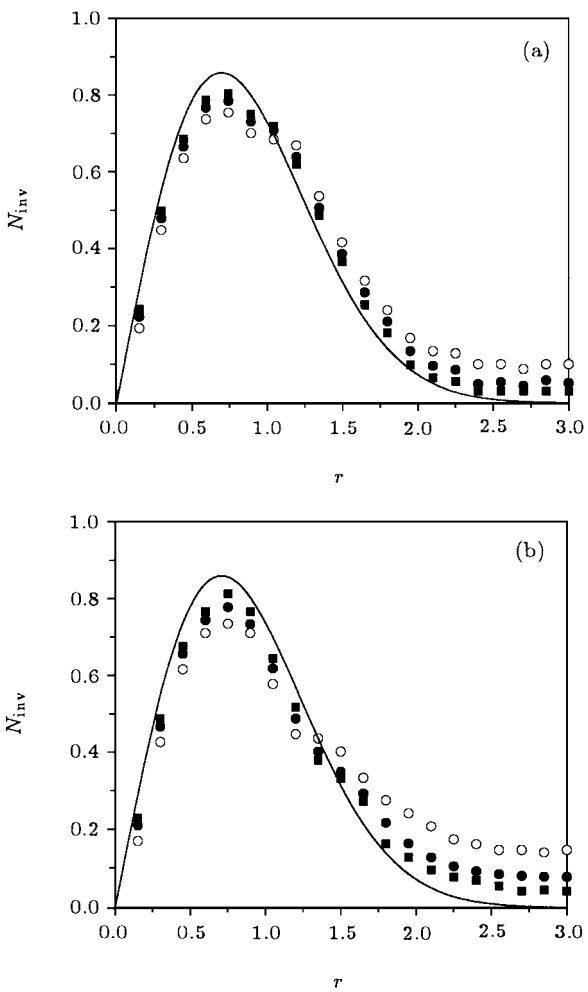



**Fig.4.** The normalized size distribution of invaded throats $N_{\rm inv}(r)$ for different values of correlation parameter ($\varepsilon$=0.8(a), 0.2(b)): ○,$P$=0.8; ●,$P$=0.9; ■, $P$=1.

These results indicate that the geometry and the topology of the porous media have strong effects on the displacement processes and the structure of VF.

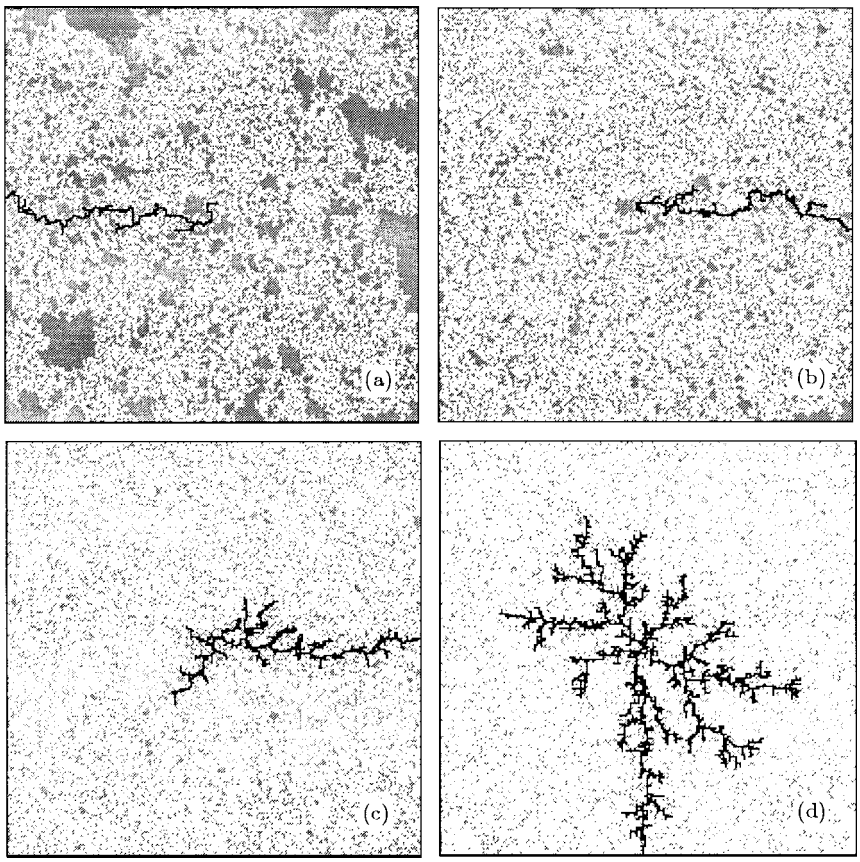



**Fig.5.** VF patterns in four different percolation clusters ((a) $P$=0.6, (b) 0.7, (c) 0.8, (d) 0.9). $\varepsilon$=0.2 and $M$=1000.

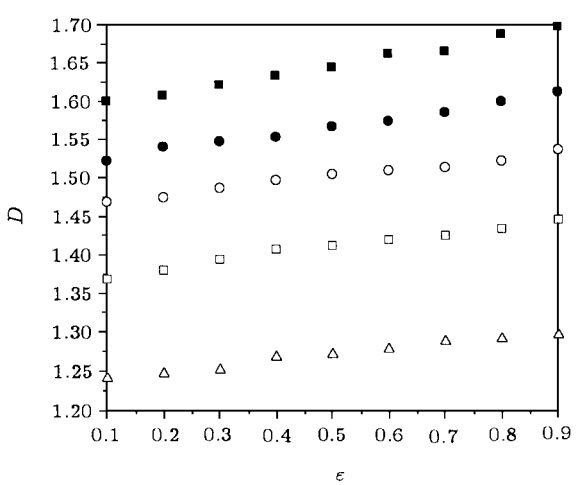



**Fig.6.** Fractal dimension $D$ as a function of correlation parameter $\varepsilon$ at $M$=1000, for $P$=0.6 (△), 0.7 (□), 0.8 (○), 0.9 (●) and 1 (■).

## 5. The velocity distribution and sweep efficiency

The results of previous studies[9,13,20] have shown that the fluid boundary is fractal, even for a finite viscosity ratio. This prompted us to measure the scaling function. In this paper, we study the distribution of velocities normal to the interface in a percolation cluster. The method has been described in detail in Ref.[19]. After each group of 100 sites has been added, all the interfacial velocities are analysed, the root-mean-square cluster radius $R_c$ is measured, and the total numbers of filled sites and surface sites are recorded. Surface sites are nodes filled with the displacing fluid, but with one or more nearest neighbours occupied by the displaced fluid. At each stage, we make a histogram of the velocity distribution, sorting the velocities into equally spaced logarithmic bins. The number $N$ in each bin, assuming the scaling hypothesis, is given by

$$Nd[\ln(V)] = R_c^{f(\alpha)}\mathrm{d}(-\alpha), \tag{8}$$

where the velocity $V$ is equal to $R_c^{-\alpha}$ and d[ln($V$)] is the width of the logarithmic bin.

Hence, $\alpha$=-ln($V$)/ln($R_c$) and d[ln($V$)]=d(-$\alpha$)ln($R_c$). This gives us a scaling function

$$f(\alpha) = \frac{\ln[N\ln(R_c)]}{\ln(R_c)}. \tag{9}$$

Figure 7 shows the effect of randomness on the velocity distributions at a viscosity ratio $M$=10 and $P$=0.8.

It is obvious that they are parabola-like curves. The curves are plotted by fitting data that are averages of 20 runs. The tail of the distribution (large $\alpha$) is longer for the larger correlation parameter $\varepsilon$. When $\varepsilon \leq 0.2$, the distribution is very sharp.

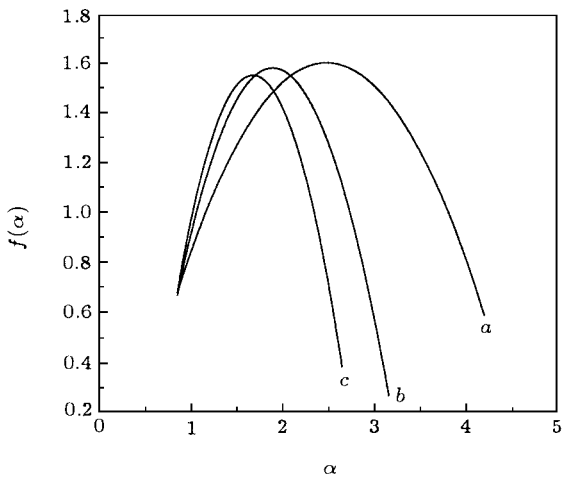



**Fig.7.** Scaling function $f(\alpha)$ and the effect of the correlation parameter $\varepsilon$: (a) $\varepsilon$=0.8; (b) $\varepsilon$=0.6; (c) $\varepsilon$=0.2.

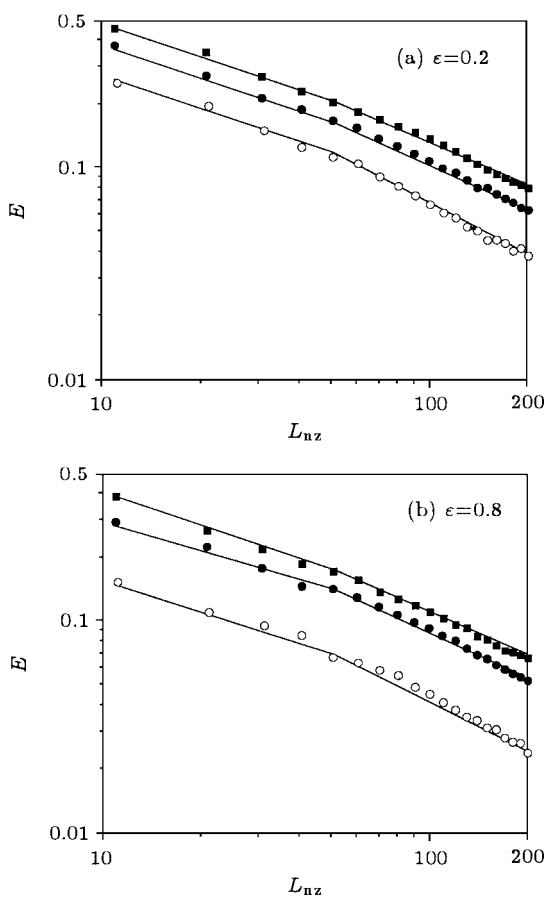



**Fig.8.** Sweep efficiency $E$ as a function of lattice size $L_{\rm nz}$ when the correlation parameter $\varepsilon$=0.8(a) and 0.6(b): ■, $M$=10; ●, $M$=100; ○, $M$=1000.

A particular use of the function is to predict the sweep efficiencies $E(=A_e/A_s)$,[4] where $A_e$ and $A_s$ are the sweep area and percolation cluster area in the sweep region, respectively. Figure 8 shows that the sweep efficiency $E$ decreases with the decrease of the correlation parameter $\varepsilon$ and the increase of the network size $L_{\rm nz}$. It is apparent that $E$ has a minimum as $L_{\rm nz}$ increases to the maximum no matter what the values of $P$, $M$ and $\varepsilon$. It must be pointed out that the $E \sim L_{\rm nz}$ curve has two linear regions. This means that the VF pattern has a frozen zone and an active zone.[20]

Our studies on some 51×51, 101×101 and 401×401 square lattices concerning finite size effects show that the above-mentioned conclusions are still tenable.

## 6. Conclusion

The porous media model constructed in this paper is the percolation cluster with varying percolation probability $P$ and correlated site–bonds. Taking into account both the pore and the throat geometry, the VF in porous media has been investigated by using the standard over-relaxed Gauss–Seidel scheme. The simulation results show that the VF structure varies with the correlation parameter $\varepsilon$, the viscosity ratio $M$ and the percolation probability $P$.

For $\varepsilon$ <1, the cluster size decreases with the decrease of $\varepsilon$. No matter what the value of $\varepsilon$, the VF pattern in a percolation cluster has an anisotropy manner. The smaller the correlation parameter $\varepsilon$, the greater the deviation of the normalized size distribution of the invaded throat $N_{\rm inv}(r)$ from the truncated Rayleigh distribution. The normalized size distribution of the invaded throat $N_{\rm inv}(r)$ shows that the major deviation occurs where $r$ is large. The normalized distribution of the size of the invaded throat $N_{\rm inv}(r)$ also greatly deviates from the truncated Rayleigh distribution for smaller $\varepsilon$. The smaller the value of $\varepsilon$, the greater the deviation. For a larger viscosity ratio $M$, the VF pattern looks like a DLA structure in the percolation cluster. The fractal dimension $D$ increases with the increase of the percolation probability $P$ and the correlation parameter $\varepsilon$. The velocity distribution $f(\alpha)$ of VF in a percolation cluster is a parabola-like curve. The tail of the distribution (large $\alpha$) is longer for a larger $\varepsilon$. For a smaller value of $\varepsilon$, the distribution is very sharp. The sweep efficiency $E$ decreases with the decrease of $\varepsilon$ and the increase of the network

size $L_{nz}$. $E$ has a minimum, as $L_{nz}$ increases to the maximum no matter what the values of $P$, $M$ and $\varepsilon$. The $E \sim L_{nz}$ curve has two linear regions (the frozen zone and the active zone). The geometry and topology of the porous media have strong effects on the displacement processes and the structure of VF.

## References


[1] Meakin P 1986 *Phys. Rev.* A **33** 4199
[2] Ben-Jacob E, Godby R and Goldenfeld N D 1985 *Phys. Rev. Lett.* **55** 1315
[3] DeGregoria A J 1985 *Phys. Fluids* **28** 2933
[4] Siddiqui H and Sahimi M 1990 *Chem. Eng. Sci.* **45** 163
[5] King P R and Scher H 1988 *Phys. Rev.* A **37** 874
[6] Szep J, Cresti J and Kertesz J 1985 *J. Phys. A: Math. Gen.* **18** L413
[7] Tian J P and Yao K L 1998 *Chin. Phys. Lett.* **15** 577
[8] Chen J D and Wilkinso D 1985 *Phys. Rev. Lett.* **55** 1892
[9] King P R 1987 *J. Phys. A: Math. Gen.* **20** L529
[10] Tian J P and Yao K L 1998 *Acta Phys. Sin.* (*Oversea Edition*) **7** 681
[11] Sahimi M 1993 *Rev. Mod. Phys.* **65** 1393
[12] Tian J P and Yao K L 1998 *Phys. Lett.* A **251** 259
[13] Tian J P and Yao K L 2000 Yao, *Eur. Phys. J.* B **14** 543
[14] Murat M and Aharony A 1986 *Phys. Rev. Lett.* **57** 1875
[15] Ferer M, Sams W N, Geisbrecht R A and Smith D H 1993 *Phys. Rev.* E **47** 2713
[16] Vidales A M, Faccio R J, Rriccardo J, Miranda E N and Zgrablich G 1995 *Physica* A **218** 19
[17] Sahimi M and Imdak A O 1988 *J. Phys. A: Math. Gen.* **21** 3833
[18] Daccord D, Nitmann J and Stanley H E 1986 *Phys. Rev. Lett.* **56** 336
[19] Blunt M J and King P R 1988 *Phys. Rev.* A **37** 3935
[20] Boularot H and Albinet G 1996 *Phys. Rev.* E **53** 5106